Exploiting Multipath from Airborne Platforms for Direction of Arrival Estimation

Marija M. Nikolic[#1,*2], Arye Nehorai[#1], *Fellow, IEEE* and Antonije R. Djordjevic[*2]

[#1] *Department of Electrical and Systems Engineering, Washington University in St. Louis, St. Louis, MO 63130 USA*

[1]mnikolic@ese.wustl.edu

[2]nehorai@ese.wustl.edu

[*2]*School of electrical Engineering, University of Belgrade, Bulevar Kralja Aleksandra 73, 11000 Belgrade, Serbia*

[3]edjordja@etf.rs

***Abstract*—In the direction-of-arrival estimation, the scattering of the incident signal from airborne platforms is often neglected or considered as a source of clutter. However, these additional signal paths, mostly due to the diffraction from the platform wedges, contain useful information about the incoming waves. Recent research showed that the waves reflected from the known objects surrounding the target improve the accuracy of the target estimation or image. We show that similar improvement is obtained if the array interaction with the hosting platform is taken into the account. We incorporate the multipath into the signal processing algorithms, and study the improvement by computing the Cramer-Rao bound. We show that the exploitation of the multipath from the sensor platforms improves the estimation accuracy significantly. Moreover, the capacity to resolve multiple incident signals is enhanced.**

I. Introduction

Radars often receive multiple signals from the target due to the reflections from the objects near the target. Several studies [1]-[6] show that the target localization is improved if the reflections from water, land, or surrounding buildings are taken into account. Additional signal paths increase the radar coverage, especially when there is no optical visibility between the radar and the target [4]. Multiply scattered waves are used to obtained different views of the target, resulting in an enhanced imaging resolution [6].

Sensor arrays are typically mounted on electrically large platforms. These platforms are also significant source of the multipath. At sufficiently high frequencies, incident electromagnetic waves scatter at several locations (scattering centers) on the platforms [7]-[11]. Sensors receive summation of the direct signal and its time-delayed echoes. Conventional direction finding systems try to suppress these signal replicas by treating them as interference. In [12] the authors considered a simple system consisting of a sensor and two nearby ideal reflectors. The inclusion of the reflectors improved the accuracy of the direction-finding algorithm. The proposed approach was inspired by the human auditory system where the multipath reflections from the external ear (pinna) enable 3D direction finding [13], [14]. However, specular reflections are not present in most realistic situations, such as antenna arrays mounted on the airborne platforms. Due to the low profile and aerodynamic shape of the aircrafts, the dominant multipath mechanism is diffraction. We show that incorporating the knowledge about the diffraction from the platform will not only improve the accuracy of the model, but also improve the estimation in the same way as the multipath close to the targets or multipath from nearby reflectors. We show that, due to the diffraction from the platform, the effective array size increases, resulting in better angular resolution of the direction finding system.

We carry out our analyses in the context of a passive sensor array mounted on the aircraft. We assume that the antennas in the array are not very directional. Hence, besides the signal radiated from the target, they receive delayed and attenuated signal echoes due to the scattering from the platform. The work in this paper also applies to a system with a narrow beam that can be steered in a variety of directions. In the latter case, it is possible to isolate data from the different paths. The net result is that the number of the parameters that can be resolved increases.

We analyze the effect of the multipath from platforms in the framework of statistical signal processing. We estimate the unknown direction of arrival (DOA) using the maximum likelihood (ML) algorithm. To study the performance improvement in the DOA estimation, we compute the Cramer-Rao bound (CRB). We show that the ability of the array to resolve multiple incident waves is significantly improved, especially when their propagation directions are slightly different. Although we consider arrays mounted on airborne platforms, the underlying principle can be applied to other kinds of sensor platforms.

The outline of the paper is as follows. We formulate the problem in Section II and detail the electromagnetic modeling. In the Section III, we explain the signal processing approach, based on the Cramer-Rao bound and maximum likelihood estimation. In the Section IV we present the results of the analysis.

II. Multipath from the Sensor Platforms

A. Problem Formulation

We assume that a plane-wave signal impinges a uniform linear array from the DOA (θ, ϕ). The time-domain waveform of the incident signal (or equivalently its spectrum) is assumed to be known. The sensor array consists of M antennas, located at $\mathbf{r}_m$, $m = 1, \ldots, M$. The induced voltage in the mth sensor can be represented as [15]

$$V(\mathbf{r}_m, f, \theta, \phi) = \mathbf{E}_{\text{inc}}(f, \theta, \phi) \cdot \mathbf{l}_{\text{eff\_env}}(\mathbf{r}_m, f, \theta, \phi) \;, \quad (1)$$

where $\mathbf{E}_{\text{inc}}(f, \theta, \phi)$ is the incident electric field at the global coordinate origin for the platform, and $\mathbf{l}_{\text{eff\_env}}(\mathbf{r}_m, f, \theta, \phi)$ is the effective electrical length of the sensor antenna that takes into account environment, i.e., it encompasses reflections and diffractions on the platform. We detail the computation of the effective length of the sensor on platform in Section IIC. We assume that the incident electric field may be represented as

$$\mathbf{E}_{\text{inc}} = AS(f)\mathbf{E}_0 , \quad (2)$$

where A is the signal amplitude, $S(f)$ is the Fourier transform of the signal waveform, and $\mathbf{E}_0$ is the polarization vector. We write the induced voltage as

$$V(\mathbf{r}_m, f, \theta, \phi) = AH(\mathbf{r}_m, f, \theta, \phi),$$
$$H = S\, \mathbf{E}_0 \cdot \mathbf{l}_{\text{eff env}} . \quad (3)$$

B. Electromagnetic Modeling

At sufficiently high frequencies, the radiated field of the antenna on the platform can be separated into the direct component and components produced by the reflection and diffraction from the platform [9]-[11]. Hence, the radiation of the mth sensor on the platform in the direction (θ, ϕ) can be represented by the sum

$$\mathbf{E}(\mathbf{r}_m, \theta, \phi) = \mathbf{E}_{\text{S}}(\theta, \phi)\exp(\mathrm{j}\beta \mathbf{r}_m \cdot \mathbf{r}_0) + \\ + \sum_{i=1}^{I} \mathbf{E}_i^{\text{r}}(\mathbf{r}_m, \theta, \phi) + \sum_{l=1}^{L} \mathbf{E}_l^{\text{d}}(\mathbf{r}_m, \theta, \phi), \quad (4)$$

where $\mathbf{E}_{\text{s}}(\theta, \phi)$ is the electric field radiated by the sensor positioned in the platform coordinate origin in the absence of the multipath (i.e., reflection and diffraction), $\mathbf{E}_i^{\text{r}}$ is the electric field reflected from the platform at the ith reflection point, $i = 1, \ldots, I$, and $\mathbf{E}_l^{\text{d}}$ is the electric field diffracted from the platform at the lth diffraction point $l = 1, \ldots, L$, and $\mathbf{r}_0$ is the unit vector pointing in the direction (θ, ϕ).

The radiated electric field given by (4) can be represented in terms of the antenna effective length following the classical formula [15]

$$\mathbf{E}(\mathbf{r}_m, \theta, \phi) = -\mathrm{j}\frac{1}{4\pi}\sqrt{\frac{\mu_0}{\varepsilon_0}}\, \underline{I}_0\, \beta\, \mathbf{l}_{\text{eff\_env}} \frac{\mathrm{e}^{-\mathrm{j}\beta r}}{r} . \quad (5)$$

Reciprocity considerations result in (1).

In this paper, we consider platforms for which the only source of the multipath is diffraction. We assume that the platforms are perfectly conducting. We compute the diffracted fields using the GTD formulation. The diffracted electric field is [16]

$$\mathbf{E}_l^{\text{d}}(\theta, \phi) = \mathbf{E}_{\text{s}}(\theta_l, \phi_l)\exp(\mathrm{j}\beta \mathbf{r}_m \cdot \mathbf{r}_0) \cdot \\ \cdot \frac{\exp(-\mathrm{j}\beta s)}{s} \cdot \overline{\mathbf{D}}\sqrt{s}\, \exp(\mathrm{j}\beta \mathbf{r}_l^{\text{d}} \cdot \mathbf{r}_0),$$

$$s = \left|\mathbf{r}_m - \mathbf{r}_l^{\text{d}}\right|, \; l = 1, \ldots, L , \quad (6)$$

where $\mathbf{r}_l^{\text{d}}$ is the location of the lth diffraction point, $\overline{\mathbf{D}}$ is the dyadic diffraction coefficient, and θ_l, ϕ_l are azimuth and elevation angles of the diffraction point. For the considered structures, higher-order diffractions are negligible.

We incorporated in our GTD model the numerical data for the radiate field of the isolated sensors (**E**s) obtained by the WIPL-D software (MoM) [17].

C. Measurement Model

We suppose K broadband signals that impinge on the array from distinct DOAs (θ_k, ϕ_k), where K is assumed to be known. The array takes measurements at uniform frequency samples f_n, $n = 1, \ldots, N$. The output of the mth sensor is, from (3),

$$x_m(f_n) = \sum_{k=1}^{K} A_k H(\mathbf{r}_m, f_n, \theta_k, \phi_k) + w_m , \quad (7)$$

where w_m is the complex white Gaussian noise with variance σ^2. The array output can be put in a compact form

$$\mathbf{x} = \mathbf{H}\mathbf{a} + \mathbf{w} ,$$
$$\mathbf{x} = \left[\mathbf{x}_1^T, \ldots, \mathbf{x}_M^T\right]^T , \; \mathbf{x}_m = \left[x_m(f_1), \ldots, x_m(f_N)\right]^T , \quad (8)$$

where $\mathbf{H}$ is the steering matrix

$$\mathbf{H} = \left[\mathbf{H}_1 \ldots \mathbf{H}_K\right], \; \mathbf{H}_k = \left[h_{1k}^T, \ldots, h_{Mk}^T\right]^T ,$$
$$h_{mk} = \left[H(\mathbf{r}_m, f_1, \theta_k, \phi_k), \ldots, H(\mathbf{r}_m, f_N, \theta_k, \phi_k)\right]^T , \quad (9)$$

and **a** is the vector with unknown signal amplitudes

$$\mathbf{a} = \left[A_1, \ldots, A_K\right]. \quad (10)$$

For simplicity, we assume that the polarization of the incoming wave is known. However, the extension to the case of the unknown polarization is straightforward. Therefore, let $\mathbf{\Theta} = [\mathbf{a}, \boldsymbol{\theta}, \boldsymbol{\varphi}]$, $\boldsymbol{\varphi} = [\phi_1, \ldots, \phi_K]$, $\boldsymbol{\theta} = [\theta_1, \ldots, \theta_K]$ be the unknown parameter vectors, where the azimuth and elevation angles are the parameters of interest.

III. Signal Processing

A. Cramer-Rao Bound

We compute the Cramer-Rao bound to demonstrate the estimation improvement due to incorporation of the multipath. The covariance matrix of any unknown parameter vector is lower-bounded by the CRB, which is attainable by statistically efficient unbiased estimators. Maximum likelihood estimation attains the CRB asymptotically. The CRB matrix is the inverse of the Fisher information matrix,

$$\mathbf{CRB} = \mathbf{I}^{-1}, \; \mathbf{I} = 2\,\mathrm{Re}\left\{\begin{bmatrix} \mathbf{I}_{\theta\theta} & \mathbf{I}_{\theta\varphi} & \mathbf{I}_{\theta\mathbf{a}} \\ \mathbf{I}_{\theta\varphi}^H & \mathbf{I}_{\varphi\varphi} & \mathbf{I}_{\varphi\mathbf{a}} \\ \mathbf{I}_{\theta\mathbf{a}}^H & \mathbf{I}_{\varphi\mathbf{a}}^H & \mathbf{I}_{\mathbf{aa}} \end{bmatrix}\right\}, \quad (11)$$

where

$$\left[\mathbf{I}_{\mathbf{aa}}\right] = \frac{1}{\sigma^2}\mathbf{H}^H\mathbf{H} , \quad (12)$$

$$[\mathbf{I}_{\theta\theta}]_{ij} = \frac{1}{\sigma^2}\mathbf{a}^H \frac{\partial \mathbf{H}}{\partial \theta_i}^H \frac{\partial \mathbf{H}}{\partial \theta_j}\mathbf{a}, \quad (13)$$

$$[\mathbf{I}_{\varphi\varphi}]_{ij} = \frac{1}{\sigma^2}\mathbf{a}^H \frac{\partial \mathbf{H}}{\partial \phi_i}^H \frac{\partial \mathbf{H}}{\partial \phi_j}\mathbf{a}, \quad (14)$$

$$[\mathbf{I}_{\theta\mathbf{a}}]_{ij} = \frac{1}{\sigma^2}\mathbf{a}^H \frac{\partial \mathbf{H}}{\partial \theta_i}^H \mathbf{H}_j \quad (15)$$

$$[\mathbf{I}_{\varphi\mathbf{a}}]_{ij} = \frac{1}{\sigma^2}\mathbf{a}^H \frac{\partial \mathbf{H}}{\partial \phi_i}^H \mathbf{H}_j, \quad (16)$$

$$[\mathbf{I}_{\theta\varphi}]_{ij} = \frac{1}{\sigma^2}\mathbf{a}^H \frac{\partial \mathbf{H}}{\partial \theta_i}^H \frac{\partial \mathbf{H}}{\partial \phi_j}\mathbf{a}. \quad (17)$$

The elements on the main diagonal of the CRB matrix contain the parameter variances.

Since there are no closed-form expressions for diffraction, we compute derivatives in (13)-(17) numerically. To obtain numerically stable results, we first approximate (3) by polynomials with respect to the azimuth and elevation angles. Then we compute analytical derivatives of the polynomial approximation.

B. *Maximum Likelihood Angle Estimation*

We estimate the unknown parameters using the maximum likelihood approach [18]-[20]. The performance of the maximum likelihood estimation is optimal for large data records, i.e., it achieves asymptotically the CRB. In the case of white Gaussian noise, which is the common model for the measurement noise, the maximum likelihood estimates of the unknown parameters are obtained by minimizing

$$\hat{\mathbf{a}}, \hat{\boldsymbol{\theta}}, \hat{\boldsymbol{\varphi}} = \arg\min_{\mathbf{a},\boldsymbol{\theta},\boldsymbol{\varphi}} \|\mathbf{x} - \mathbf{H}\mathbf{a}\|^2, \quad (18)$$

where $\|\cdot\|^2$ denotes the Euclidian norm. The loss function (18) can be explicitly minimized with respect to **a**, which yields [18]

$$\hat{\mathbf{a}} = \left(\mathbf{H}^H\mathbf{H}\right)^{-1}\mathbf{H}^H\mathbf{x}, \quad (19)$$

$$\hat{\boldsymbol{\theta}}, \hat{\boldsymbol{\varphi}} = \arg\min_{\boldsymbol{\theta},\boldsymbol{\varphi}} \|\mathbf{x} - \mathbf{H}\hat{\mathbf{a}}\|^2 = \arg\min_{\boldsymbol{\theta},\boldsymbol{\varphi}} \mathbf{x}^T \Pi_{\mathbf{H}}^{\perp}(\boldsymbol{\theta},\boldsymbol{\varphi})\mathbf{x}, \quad (20)$$

where

$$\Pi_{\mathbf{H}}^{\perp} = \mathbf{I} - \mathbf{H}\left(\mathbf{H}^H\mathbf{H}\right)^{-1}\mathbf{H}^H, \quad (21)$$

is the orthogonal projection matrix of the null space of **H**. Therefore, the unknown DOAs are computed by performing $2K$ nonlinear minimizations.

IV. Multipath from UAV

In this section, we study the performance improvement resulting from the exploitation of the multipath due to the diffraction from UAV Predator, shown in Fig. 1. The Predator is a medium-altitude, long endurance unmanned aerial vehicle system (UAV = Unmanned Aerial Vehicle). The airplane is 8.1 m long with 14.8 m wing span. The main sources of diffraction are wings, tail, and wedges at the bottom of the aircraft. In our computations, we used the geometrical model of the Predator provided by [21].

To evaluate the improvement in the DOA estimation, we compute the CRB. For comparison, we also consider the DOA estimation in the case without the multipath, i.e., in the case where the sensors are mounted above an infinite ground plane.

We assume that the incident signal has a flat spectrum over the frequency band $W = [0.9 \text{ GHz}, 1.1 \text{ GHz}]$, i.e., $S(f) = 1$ for all frequencies within W, otherwise $S(f) = 0$. We set $A = 1$ and $\mathbf{E}_0 = \mathbf{i}_\theta$. The resonant frequency of the sensors is $f_0 = 1$ GHz. The sensors take measurements at $N = 20$ uniform frequency samples in the considered frequency range.

We perform the DOA estimation using the uniform linear array of $M = 7$ half-wavelength spaced monopoles. The array is located along the Predator symmetry axis, which coincides with y-axis of the adopted coordinate system (Fig. 1 and Fig. 2).

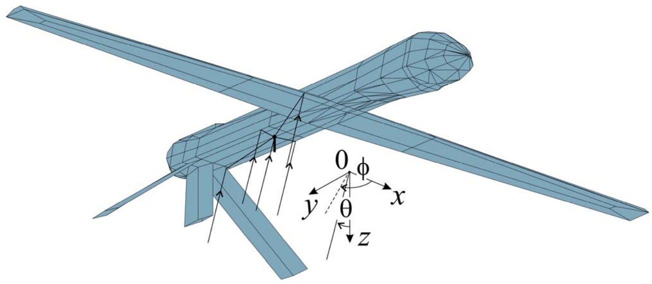

Fig 1. Geometrical model of Predator, and adopted coordinate system.

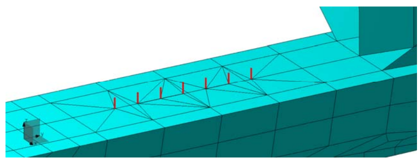

(a)

Fig. 2. Uniform linear array of 7 half-wavelength spaced monopoles mounted on the Predator.

We consider a plane wave incident on the UAV. Let $\boldsymbol{\Theta} = [A, \theta, \phi]$ be the unknown parameter vector, where the azimuth and elevation are the parameters of interest. We compute the CRB for the unknown parameters for a wide range of incident directions. In the computations, we set $\sigma^2 = 0.01$. The results are shown in Fig. 3 (red color). In the same figure, we showed the results for the case without the multipath, i.e., when the array is mounted above the infinite ground plane (gray color).

The multipath improves the accuracy of the angle estimation for all considered directions. The lower bound on the mean square error is almost uniform everywhere.

In the case of no multipath, the DOA estimation suffers from large inaccuracies for the directions for which the radiation pattern of the sensors does not have large variations.

We computed the maximum likelihood estimates for the DOA using 20 independent Monte Carlo simulations. In Fig. 4, we show that the ML estimates are very close to the best unbiased estimates. The discrepancies between the RMSE and the lower bound on the RMSE, i.e., the sharp peaks in Fig. 4, correspond to directions for which the signal-to-noise ratio (SNR) is about 0 dB. Hence, there is a threshold for SNR above which the performance of the MLE asymptotically approaches the CRB.

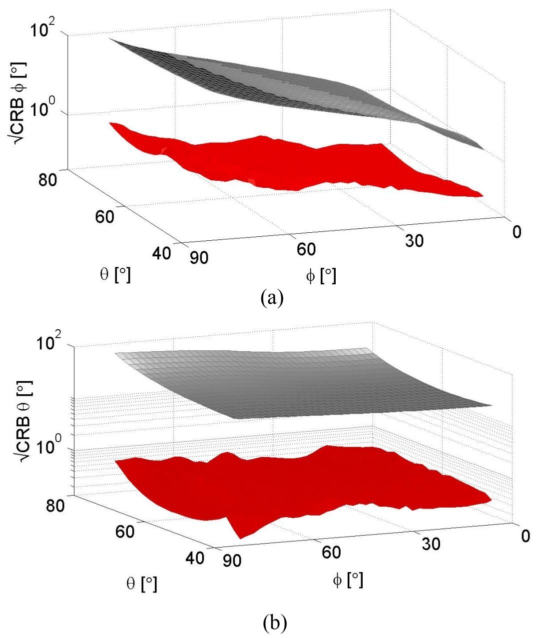

Fig. 3. Square root of the CRB for (a) elevation and (b) azimuth. The results are shown in log scale. Computations are performed for the array mounted on the Predator (red color) and the PEC (grey color).

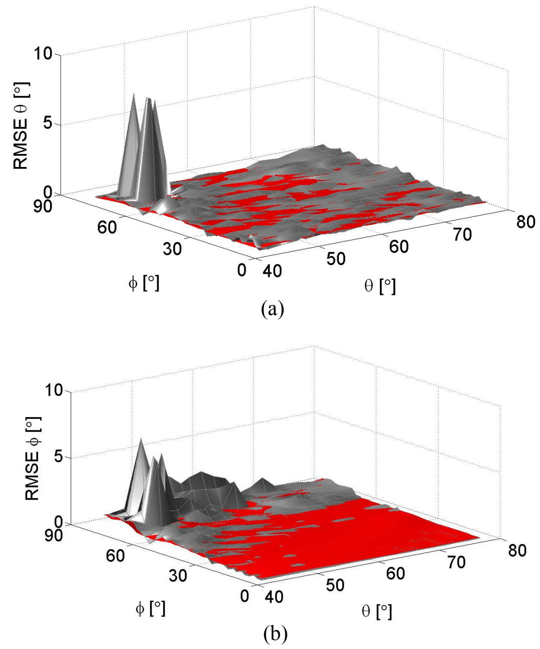

Fig. 4. The root-mean-square error (grey color) for the maximum likelihood estimates of the (a) elevation and (b) azimuth. Results are obtained using 20 independent Monte Carlo simulations. For comparison, the square root of the CRB is shown (red color).

V. Conclusions

We showed that the multipath due to the interaction between the sensor array and the hosting platform provides significant information on the direction of arrival of the impinging electromagnetic waves. The exploitation of the multipath improves the accuracy of the estimation of the direction of arrival, which is of the particular interest in the case of limited array apertures. The improvement is better for electrically large platforms with several scattering centers. The results we obtained are in the agreement with recent studies showing that the resolution of the radar images is improved if the multipath from known objects in the vicinity of targets is taken into account.

We analyzed the contribution of the multipath on the performance of the estimation in the context of the maximum likelihood estimation. We computed the Cramer-Rao bound as a performance measure to study the DOA estimation accuracy. The additional signal paths reduced the minimal variances of the unknown parameters. The gain was significant although the only source of the multipath was diffraction.

Detailed analysis is performed for small sensors with wide beamwidth. However, the results also apply to sensors with narrow beams and direction-agile radiation patterns.

Acknowledgment

This work was supported in part by the Department of Defense under the Air Force Office of Scientific Research MURI Grant FA9550-05-1-0443, ONR Grant N000140810849, DARPA Grant HR0011-07-1-0036, and by COST Action IC0603 (Assist).

References

[1] T. Lo, J. Litva, "Use of a highly deterministic multipath signal model in low-angle tracking," *IEE Proceedings-F Radar and Signal Processing*, vol.138, no.2, pp.163-171, Apr 1991.

[2] M. Skolnik, G. Andrews, J.P. Hansen, "Ultrawideband microwave-radar conceptual design," IEEE Aerospace and Electronic Systems Magazine, vol.10, no.10, pp.25-30, Oct 1995.

[3] C.D. Berube, P.R. Felcyn, K. Hsu, J. H. Latimer II, D.B. Swanay, "Target Height Estimation using Multipath Over Land", The MITRE Corporation, 202 Burlington Road, Bedford, MA 01730.

[4] J.L. Krolik, J. Farrell, and A. Steinhardt, "Exploiting Multipath Propagation for GMTI in Urban Environments," *IEEE Conference on Radar*, April 2006.

[5] Multipath Exploitation Radar Industry Day, Darpa, August 2007.

[6] C.J. Nolan, M. Cheney, T. Dowling, R. Gaburro, "Enhanced angular resolution from multiply scattered waves," *Inverse Problems*, vol. 22., pp. 1817-1834, 2006.

[7] Carriere, R.; Moses, R.L., "High resolution radar target modeling using a modified Prony estimator," *IEEE Transactions on Antennas and Propagation*, vol.40, no.1, pp.13-18, Jan 1992.

[8] Potter, L.C.; Da-Ming Chiang; Carriere, R.; Gerry, M.J., "A GTD-based parametric model for radar scattering," *IEEE Transactions on Antennas and Propagation*, vol.43, no.10, pp.1058-1067, Oct 1995.

[9] R. Bhalla, H. Ling, "Three-dimensional scattering center extraction using the shooting and bouncing ray technique," *IEEE Transactions on Antennas and Propagation*, vol.44, no.11, pp.1445-1453, Nov 1996.

[10] M. Hurst, R. Mittra, "Scattering center analysis via Prony's method," *IEEE Transactions on Antennas and Propagation*, vol.35, no.8, pp. 986-988, Aug 1987.

[11] L. Qing Li, E.J. Rothwell, C. Kun-Mu Chen; D.P. Nyquist, "Scattering center analysis of radar targets using fitting scheme and genetic algorithm," *IEEE Transactions on Antennas and Propagation*, vol.44, no.2, pp.198-207, Feb 1996.

[12] S. Sen and A. Nehorai, “Exploiting close-to-the-sensor multipath reflections using a human-hearing-inspired model,” to appear in *IEEE Trans. on Signal Processing*.

[13] D. W. Batteau, “The role of the pinna in human localization,” in *Proc. of the Royal Society of London*, Series B, Biological Sciences, vol. 168, no. 1011, Aug. 15 1967.

[14] S. Sen and A. Nehorai, "Performance analysis of 3D direction estimation based on head-related transfer function," to appear in *IEEE Trans. on Audio, Speech and Language Processing.*

[15] C.A. Balanis, *Antenna Theory: Analysis and Design*, Wiley, New York, 1997.

[16] R. G. Kouyoumjian and P. H. Pathak, “A uniform geometrical theory of diffraction for an edge in a perfectly conducting surface,” *Proc. IEEE*, vol. 62, pp. 1448-1461, November 1974.

[17] B. Kolundžija, J. Ognjanović, T. Sarkar, M. Tasić, D. Olćan, B. Janić, and D. Šumić, *WIPL-D Pro. v5.1*, WIPL-D, 2004.

[18] Nehorai, A.; Paldi, E., “Vector-sensor array processing for electromagnetic source localization,” *IEEE Transactions on Signal Processing*, vol.42, no.2, pp.376-398, Feb 1994.

[19] Li, J.; Compton, R.T., Jr., “Maximum likelihood angle estimation for signals with known waveforms,” *IEEE Transactions on Signal Processing*, vol.41, no.9, pp.2850-2862, Sep 1993.

[20] Stoica, P.; Sharman, K.C., “Maximum likelihood methods for direction-of-arrival estimation,” *IEEE Transactions on Acoustics, Speech and Signal Processing,* vol.38, no.7, pp.1132-1143, Jul 1990.

[21] 3D Studio, www.The3dStudio.com.